Binding and transport properties of a benzo[*b*]thiophene-based mono-(thio)urea library

Cristina Moiteiro,[a] Igor Marques,[b] William G. Ryder,[c] Vasco Cachatra,[a] Sílvia Carvalho,[a] Li-Jun Chen,[c] Brian J. Goodfellow,[b] Philip A. Gale*,[c][d] and Vítor Félix*[b]

[a] Prof. C. Moiteiro, V. Cachatra, Dr. S. Carvalho,
Centro de Química Estrutural, Faculdade de Ciências,
Universidade de Lisboa, Campo Grande, 1749-016 Lisboa (Portugal)
[b] Dr. I. Marques, Prof. B. J. Goodfellow, Prof. V. Félix
CICECO – Aveiro Institute of Materials, Department of Chemistry,
University of Aveiro, 3810-193 Aveiro (Portugal)
E-mail: vitor.felix@ua.pt
[c] W. G. Ryder, Dr. L.-J. Chen, Prof. P. A. Gale
School of Chemistry (F11), The University of Sydney
Sydney, NSW 2006 (Australia)
E-mail: philip.gale@sydney.edu.au
[d] Prof. P. A. Gale
The University of Sydney Nano Institute (SydneyNano), The University of Sydney
Sydney, NSW 2006 (Australia)

Supporting information for this article is given via a link at the end of the document.

Abstract: Using the chemical versatility of the benzo[*b*]thiophene motif, an extensive library of 24 (thio)urea receptors, with different binding properties and lipophilicities was prepared and included α,α-, α,β-, β,β-, β,γ-, α,γ-, and γ,γ-benzo[*b*]thiophene positional isomers, as well as β- or γ-benzo[*b*]thiophene-based molecules decorated with aliphatic chains or aryl moieties with different fluorination degrees. ^{1}H NMR titrations, X-ray crystallography studies, and DFT calculations showed that the receptors with higher chloride binding affinities were the β,β- and γ,γ-bis-benzo[*b*]thiophene and fluorinated aryl β- or γ-benzo[*b*]thiophene derivatives that synergistically bind chloride with the urea and one or two $C_{β/γ}$-H ancillary binding groups. Experimental efflux studies showed that, among these small drug-like molecules, only the highly fluorinated analogues displayed anion transmembrane transport activity, suggesting that this property is dependent on the receptors' lipophilicity and hydrogen bonding ability. Moreover, LUV based assays, undertaken under electroneutral and electrogenic conditions, together with NMDG-Cl assays, indicated that anion efflux occurs mainly through an uniport mechanism. Further MD simulations showed that anion transport is highly dependent on the orientation and interactions of the receptors at the water/lipid interface.

Introduction

Many important physiological functions depend on the balance of solution concentrations across cell membranes, and may involve ions with biological relevance.[1] This delicate equilibrium is typically managed by integral membrane proteins that function as selective ion channels. Their malfunction leads to diseases, classified as channelopathies, such as cystic fibrosis, associated with a deficiency in the transport of chloride.[1-2] The need for drug-like molecules with the potential to become “channel replacement therapies”[2-3] has been one of the main driving forces behind the development of synthetic anion transporters over the last few decades.[2] Moreover, the pharmaceutical potential of these small molecules also extends to anticancer,[4] as well as to antibacterial activity.[5]

We have recently developed a series of seventeen *o*-phenylenediamine-based bis-urea molecules decorated with thiophene or benzo[*b*]thiophene motifs.[6] The binding affinity and transmembrane transport ability of these molecules for chloride were comprehensively investigated by experimental and theoretical methods. Remarkably, the spatial binding disposition of the benzo[*b*]thiophene units dictated the anion binding affinity, with the β- and γ-benzo[*b*]thiophene based receptors having association constant values for chloride that are almost twice as large as the values determined for the α-benzo[*b*]thiophene isomers.[6] While the α-benzo[*b*]thiophene derivatives adopted an extended conformation and recognised chloride only through four hydrogen bonds from the urea binding units, the β- and γ-benzo[*b*]thiophenes derivatives displayed two additional synergetic non-classical C-H hydrogen bonds from the nearby benzo[*b*]thiophene aromatic fragments. This allowed the β- and γ-benzo[*b*]thiophene derivatives to standout in chloride transport across a phospholipid bilayer model (POPC), functioning as very efficient anion carriers.

Pursuing our search for small molecules with anion transmembrane transport properties, and to further rationalise the role of the benzo[*b*]thiophene decorating motifs, we have developed a new chemical library of twenty-four benzo[*b*]thiophenes based receptors with one or two heterocyclic rings directly attached to a single (thio)urea binding unit. Moreover, the molecules in this series were designed to have distinct lipophilic characteristics, and different chloride binding strengths. Thus, the β- and γ-benzo[*b*]thiophene based molecules **1**-**8** were appended with *n*-butyl or *n*-hexyl aliphatic chains and are able to form a single C-H···Cl^- bonding contact (see Scheme 1), while **9**-**18**, obtained by a combinatorial approach using two α-, β- and/or γ-benzo[*b*]thiophene moieties (see Scheme 2), establish a different number of putative C-H···Cl^- bonding interactions: two (**9**-**13**), one (**14**-**16**) or none (**17** and **18**). Compounds **19**-**24** have β- or γ-benzo[*b*]thiophene motifs coupled with a functionalised phenyl moiety through a urea binding group. However, while in **19** and **24** the phenyl moiety contains two lipophilic electron-withdrawing -CF_3 groups, in **20**-**23**, the aryl entity is decorated with an ester *n*-butyl chain and different fluorination degrees. These small-receptors, primarily designed for anion transmembrane transport studies, also allow the evaluation of

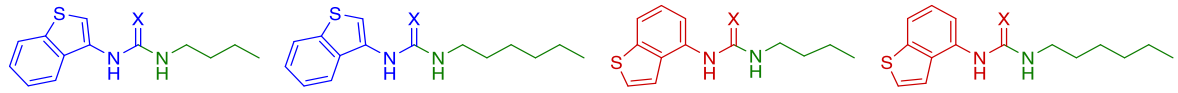

1 X= O
2 X= S

3 X= O
4 X= S

5 X = O
6 X = S

7 X = O
8 X = S

Scheme 1. β- and γ-benzo[*b*]thiophene-based (thio)ureas decorated with *n*-butyl or *n*-hexyl chains.

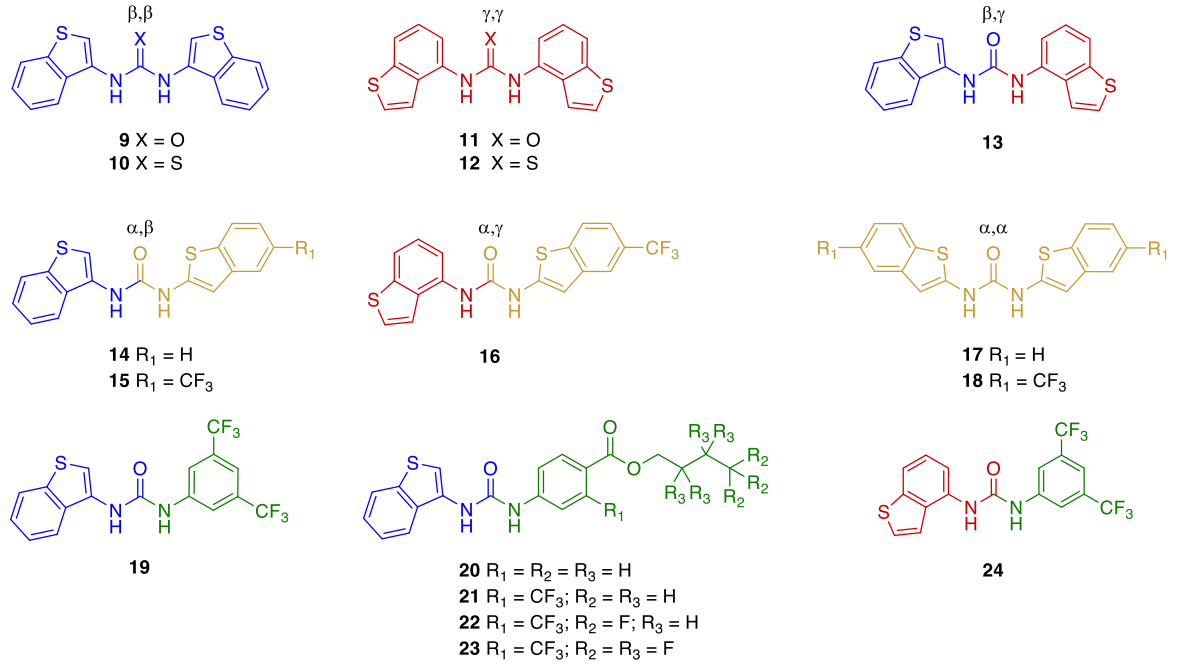

9 X = O
10 X = S

11 X = O
12 X = S

13

14 R_1 = H
15 R_1 = CF_3

16

17 R_1 = H
18 R_1 = CF_3

19

20 R_1 = R_2 = R_3 = H
21 R_1 = CF_3; R_2 = R_3 = H
22 R_1 = CF_3; R_2 = F; R_3 = H
23 R_1 = CF_3; R_2 = R_3 = F

24

Scheme 2. Isomeric bis-benzo[*b*]thiophene (thio)ureas and β- and γ-benzo[*b*]thiophene-based ureas linked to aryl motifs with different fluorination degrees.

Table 1. Log P values and chloride association constants for mono-(thio)urea benzo[b]thiophene-based receptors, relevant quantum binding descriptors, together with anion efflux data.

Compound	log P[a]	K_a (M^{-1})[b]	$V_{S,max}$[c]	ΔE (kcal mol^{-1})[d]	EC_{50} (mol%)[e]	k_{ini} (% s^{-1})[f]
Aliphatic β-benzo[*b*]thiophenes						
1	3.30	29	73.7	-9.7	-[g]	0.0426
2	4.03	60	80.1	-10.2	-[g]	-[h]
3	4.09	36	73.7	-9.7	-[g]	0.0325
4	4.83	38	80.0	-10.2	-[g]	0.0707
Aliphatic γ-benzo[*b*]thiophenes						
5	3.30	33	74.4	-9.8	-[g]	0.0222
6	4.03	35	78.0	-9.8	-[g]	0.0792
7	4.09	38	74.3	-9.2	-[g]	0.0373
8	4.83	41	77.9	-9.8	-[g]	0.0554
β,β-benzo[*b*]thiophenes						
9	5.00	254	84.7	-12.6	-[g]	0.0269
10	5.73	124	86.1	-11.3	2.0026	0.1790
γ,γ-benzo[*b*]thiophenes						
11	5.00	209	84.0	-12.2	-[g]	0.0276
12	5.73	56	83.2	-11.1	-[g]	0.0610
β,γ-benzo[*b*]thiophene						
13	5.00	199	84.7	-12.5	3.5671	0.0978
α,β-benzo[*b*]thiophenes						
14	4.92	125	89.1	-12.5	-[g]	0.0781
15	5.80	180	93.9	-12.9	0.8219	0.3367
α,γ-benzo[*b*]thiophenes						
16	5.80	175	94.1	-12.9	6.3563	0.1610
α,α-benzo[*b*]thiophenes						
17	4.85	54	92.5	-12.4	-[g]	0.0058
18	6.61	85	101.8	-13.0	-[g]	0.0039

Aryl β-benzo[*b*]thiophenes						
19	6.02	160	94.4	-12.9	0.4240	0.4163
20	5.61	219	87.9	-12.2	-[g]	0.0781
21	6.49	162	91.8	-12.8	11.1277	0.1610
22	6.75	309	93.1	-12.9	5.2830	0.1757
23	7.93	199	95.1	-13.0	7.0825	0.1389
Aryl γ-benzo[*b*]thiophene						
24	6.02	139	94.9	-12.9	1.1600	0.2685

[a] ChemAxon log P;[7] [b] Cl^- added as TBA salt and the binding constants were determined by ^1H NMR titrations in DMSO-d_6/0.5% H_2O at 293 K with BindFit (fitting error < 3%);[8] [c] Most positive value of the electrostatic potential mapped on the molecular surface (*vide infra*); [d] Interaction energy, obtained as: $\Delta E = E_{complex} - E_{receptor} - E_{anion}$ (*vide infra*, as well as Table S5); [e] EC_{50} defined as the effective concentration needed for 50% activity at t = 270 s; [f] The initial rates of chloride transport (k_{ini}) obtained by standard Cl^-/NO_3^- antiport assay for each transporter (1 mol%); [g] EC_{50} not determined due to the low transport activity; [h] k_{ini} not determined.

the impact of the activation of a N-H binding unit by an aryl moiety on the binding ability of β- and γ-benzo[*b*]thiophene-based ureas. In this paper, we report the results of a synergetic study undertaken by theoretical and experimental methods with a series of mono-(thio)urea benzo[*b*]thiophene-based receptors. This comprehensive study started with the syntheses and structural characterisation of twenty-four new molecules. Subsequently, the affinity of each small molecule for chloride was evaluated by ^1H NMR titrations, and further investigated by X-ray crystallography and by extensive DFT calculations for the chloride complexes. The ability of these small drug-like molecules, with logP values ranging between 3.3 and 7.9 (see Table 1), to facilitate chloride transmembrane transport was investigated using several selected experimental assays. Molecular Dynamics (MD) simulations were also performed to understand how these molecules passively diffuse across phospholipid bilayers to promote chloride efflux.

Results and Discussion

Synthesis The library of twenty-four benzo[*b*]thiophene-based (thio)ureas was built by the addition of aliphatic or aromatic amines to isomeric benzo[*b*]thiophene isocyanates or isothiocyanates. The isocyanates used to produce the monoureas were obtained from the α-, β- or γ-isomeric benzo[*b*]thiophene carboxylic acids via thermal Curtius rearrangement of the corresponding acyl azide. The isothiocyanate derivatives requested to yield the thioureas were synthetised by the oxidation of β- and γ-benzo[*b*]thiophene amines with 1,1'-thiocarbonyldi-2,2'-pyridone (TCP). Moreover, the asymmetrical β- and γ-benzo[*b*]thiophene (thio)ureas **1**-**8** were obtained using *n*-butyl- and *n*-hexylamines, while the corresponding aryl ureas **19** and **24** were prepared using 3,5-bis-(trifluoromethyl)amine. In contrast with these three amine reagents, which were directly used as provided by the chemical suppliers, the aryl amines functionalised with ester alkyl chains with different fluorination degrees used to prepare asymmetrical ureas **20**-**23** were previously obtained from 4-nitrobenzoic acid (**20**) and 4-nitro-2-(trifluoromethyl)benzoic acid (**21**-**23**) following the synthetic route outlined in Scheme S4. Akin to a Lego approach, the reaction between β- or γ-benzo[*b*]thiophene amines and α-, β- or γ-benzo[*b*]thiophene iso(thio)cyanates yielded the isomeric (thio)urea bis-benzo[*b*]thiophene derivatives β,β- (**9** and **10**), γ,γ- (**11** and **12**), β,γ-**13**, α,β- (**14** and **15**) and α,γ-**16**. The symmetrical α,α-benzo[*b*]thiophene monoureas were obtained by the reaction between the benzo[*b*]thiophene-2-isocyanate (**17**) or 5-(trifluoromethyl)-benzo[*b*]thiophene-2-isocyanate (**18**), and the corresponding amines were generated *in situ* through decomposition by hydrolysis of these highly reactive intermediates. Full synthetic details of all compounds are reported in the Supporting Information together with the structural characterisation data.

Binding studies The chloride binding properties of the benzo[*b*]thiophene-based mono-(thio)ureas were investigated in DMSO-d_6/0.5% H_2O solvent media at 293 K through ^1H NMR experiments. The ^1H NMR spectra, obtained during titrations of the twenty-four mono-(thio)urea receptors with tetrabutylammonium chloride, are presented in Figures S29 to S52. Overall, all titration spectra show both N-H (thio)urea resonances, together with the resonances of the C_γ-H and C_β-H in the β- and γ-benzo[*b*]thiophene derivatives. The binding association constants were determined with the BindFit software,[8] using the observed variations in chemical shifts of the N-H (thio)urea protons. Non-linear regression analyses (Figures S29 to S52) indicated that all chloride complexes display a 1:1 stoichiometry, with the binding constants reported in Table 1.

At the start of the titrations for the aliphatic-benzo[*b*]thiophene ureas (**1**, **3**, **5**, and **7**), the resonances of the N_β-H or N_γ-H protons appear at lower field, followed by the benzo[*b*]thiophene C_γ-H or C_β-H protons and by the N_{aliph}-H protons resonances at higher field. In the thiourea analogues (**2**, **4**, **6**, and **8**), the C-H and the N_{aliph}-H resonances switch places when compared with the above chemical shifts sequence. In the ^1H NMR spectra of the symmetrical β,β- (**9** and **10**) and γ,γ- (**11** and **12**) benzo[*b*]thiophene (thio)urea-based receptors, as well as in the asymmetrical β,γ-benzo[*b*]thiophene urea **13**, the N_β-H and N_γ-H protons are more downfield shifted compared to those for C_γ-H and C_β-H. In the receptors incorporating α-benzo[*b*]thiophene motifs (**14**-**18**), the N_α-H protons are heavily deshielded exhibiting the highest downfield shifts among the N-H resonances. Accordingly, in the asymmetrical α,β- (**14** and **15**) and α,γ-**16** benzo[*b*]thiophene derivatives, the N_β-H/N_γ-H resonance appears at lower field followed by those for the C_γ-H/C_β-H protons. In the aryl-benzo[*b*]thiophene ureas (**19**-**24**), the resonances of N_{arom}-H occur at lower field, followed by N_β-H or N_γ-H protons and C_γ-H or C_β-H benzo[*b*]thiophene resonances, in agreement with the chemical shift sequence observed for the remaining receptors in this library. Upon addition of chloride, the downfield chemical shifts of each small receptor follow one of sequences: N_{aliph}-H > N_β-H/N_γ-H > C_γ-H/C_β-H (**1**-**8**), N_β-H/N_γ-H > C_γ-H/C_β-H (**9**-**13**), N_α-H>N_γ-H/N_β-H > C_γ-H/C_β-H (**14**-**16**) or N_{arom}-H > N_β-H/N_γ-H > C_γ-H/C_β-H (**19**-**24**).

The aliphatic urea receptors display equivalent binding affinities for chloride, with association constants ranging between 29 and 38 M^{-1}, for β,alkyl-**1** and γ,hexyl-**7**, respectively. The thiourea receptors recognise chloride with comparable strengths, with exception of **2** with a binding affinity approximately twice as large as for its urea analogue **1**. The Lego-like replacement of the aliphatic chains on the mono-ureas skeleton by a β-,γ- or α-benzo[*b*]thiophene motif leads to a significant increase in the receptor's affinity for chloride, as shown by the binding constants of β,β-**9**, γ,γ-**11**, β,γ-**13**, and α,β-**14** isomeric bis-benzo[*b*]thiophene ureas, with values ranging between 125 and 254 M^{-1} for **14** and **9**, respectively (see Table 1). On the other hand, the isomeric α,α-benzo[*b*]thiophene urea **17**, with a binding constant of 54 M^{-1}, has the lowest affinity for chloride among the non-fluorinated bis-benzo[*b*]thiophene derivatives. Nevertheless, in this subset, **17** displays the highest acidic character for its N-H urea binding sites, as suggested by the large downfield shift of these protons in the ^{1}H NMR spectrum and electrostatic potential calculations (*vide infra*). Thus, this comparison reveals that chloride recognition by the urea binding unit is synergistically aided by two C_γ-H and/or C_β-H binding sites in **9**, **13** and **11** and one C_β-H binding site in **14**, while **17** binds the anion only through the urea N-H binding sites. The relevance of the putative C-H···Cl^- contacts to the chloride binding affinity is also evident when the association constants determined for α,β-**15** and α,γ-**16** receptors are compared with α,α-**18** benzo[*b*]thiophene derivative, even though the binding strength of the urea N-H binding sites, relatively to the previous subset, is naturally enhanced by the fluorination of the α-benzo[*b*]thiophene decorating motifs. Accordingly, **15** and **16** display similar affinity for chloride with binding constants around 180 M^{-1}, while the association constant for the symmetrical receptor **18**, with the urea binding unit activated by two α-benzo[*b*]thiophenes derivatised with a -CF_3 electron-withdrawing substituent, is only 86 M^{-1}.

Of note, the β,β-**10** and γ,γ-**12** bis-benzo[*b*]thiophene thioureas with binding constants of 124 and 55 M^{-1}, respectively, have lower binding affinity for chloride relatively to their β,β-**9** and γ,γ-**11** urea analogues (254 and 209 M^{-1}). These binding data suggest that both thiourea complexes should have distorted binding geometries with weaker convergent C-H···Cl^- bonding contacts, and, hence, a decrease in the chloride binding strength is expected as thoroughly investigated by subsequent DFT calculations (*vide infra).*

The β-benzo[*b*]thiophene ureas linked to an aromatic moiety derivatised with an ester butyl chain, **20**-**23**, have binding constants over a wide range of values between 162 M^{-1} for **21** and 309 M^{-1} for **22**. Unexpectedly, the values of the association constants for the aryl β-benzo[*b*]thiophene based receptor subset do not follow the increasing fluorination of the butyl chain or of the aromatic ring. The β-benzo[*b*]thiophene **19** derivative, with the anion affinity of urea N-H binding sites increased by the electron-deficient 3,5-trifluoromethylphenyl decorating motif, has a binding constant identical to **21**, while its γ-benzo[*b*]thiophene isomer analogue **24** has a slightly lower binding constant, with a value of 139 M^{-1}. Moreover, when compared with fluorinated receptors **15** and **16**, **19** and **24** have slightly lower binding affinities for chloride.

Theoretical insights into chloride binding affinity The binding ability of our library of (thio)urea receptors was further evaluated via a detailed molecular modelling study using Density Functional Theory (DFT) calculations carried out with Gaussian 09[9] at the PBE0-D3/6-311++G(3df,3dp) theory level and using the Conductor-like Polarizable Continuum Model (CPCM) to describe DMSO solvent effects. See ESI for further details.

The ^{1}H NMR binding studies (*vide supra*) showed that the α-, β- and γ-benzo[*b*]thiophene (thio)urea motifs recognise chloride thorough the binding modes presented in Scheme 3, in agreement with the experimental and theoretical findings previously observed for chloride complexes of benzo[*b*]thiophene-based bis-ureas.[6] Therefore, the geometry of the chloride complexes **1**-**24** were computed for a single binding scenario, with the receptors adopting their putative binding conformations shown in Scheme 1.

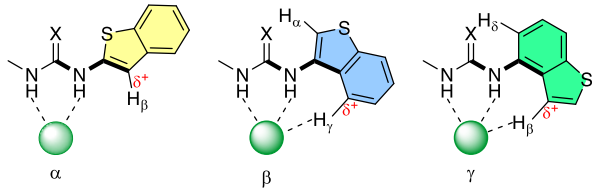

Scheme 3. Putative binding dispositions afforded by the linkage of benzo[*b*]thiophene ring through the α-, β- or γ-carbon atom to the (thio)urea binding unit, with the three bonds used to define the ξ parameter (C-N-C-C dihedral angle) highlighted in bold.

The initial hydrogen bonds between the chloride and the (thio)urea binding units were maintained in the twenty-four optimised structures, as well as the one or two ancillary hydrogen bonding contacts established between the anion and the C_γ-H and C_β-H polar bonds from the β- and γ-benzo[*b*]thiophene decorating motifs, respectively. These structural features are illustrated in Figure 1 with the computed chloride complexes of β,β- (**9**, **10**), γ,γ-benzo[*b*]receptors (**11**, **12**) symmetrical receptors, and in Figure 2 with the structures of the chloride complexes of α-benzo[*b*]thiophene-based urea derivatives α,α-**18**, α,β-**15**, and α,γ-**16** benzo[*b*]thiophene receptors. The optimised structures of the chloride complexes of the remaining receptors in our library are depicted in Figures S53 and S54.

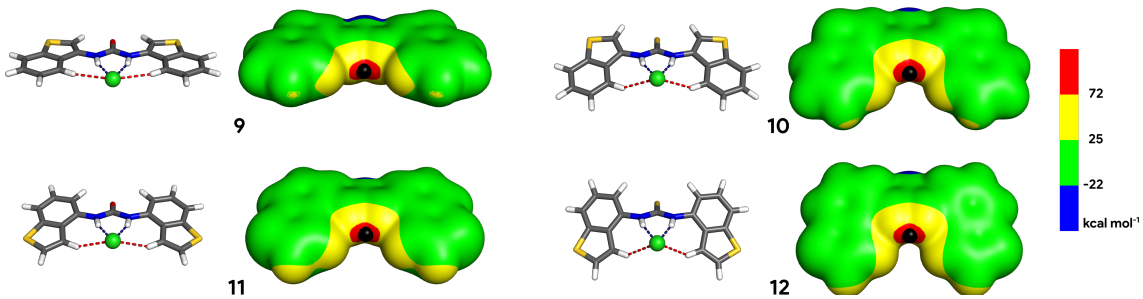

Figure 1. DFT optimised structures between the β,β- (**9**, **10**) and γ,γ- (**11**, **12**) bis-benzo[*b*]thiophene derivatives and chloride, with the anion being recognised by two N-H···Cl- hydrogen bonds from the (thio)urea binding unit (blue dashed lines), aided by two C-H···Cl- interactions from the β- or γ-benzo[*b*]thiophene fragments

(red dashed lines). Each DFT optimised structure is accompanied by the respective distribution of electrostatic potential mapped onto the molecular surface of the receptor, at 0.001 eBohr^{-1} contour.

Table 2. Average N-H···Cl$^-$ and C-H···Cl$^-$ dimensions calculated for the chloride complexes of twenty-four benzo[*b*]thiophene-based receptors, together with the average ξ torsional angles, grouped by binding unit (urea or thiourea) and by its decorating motif.[a]

Binding unit	Decorating motif	N-H···Cl$^-$		C-H···Cl$^-$		ξ torsional angle (°)
		Distance (Å)	Angle (°)	Distance (Å)	Angle (°)	
Urea	α-benzo[*b*]thiophene	3.152 ± 0.012	160.0 ± 1.8	-	-	180.0 ± 0.0
	β-benzo[*b*]thiophene	3.241 ± 0.016	159.4 ± 1.1	3.785 ± 0.031	162.9 ± 0.8	179.7 ± 0.5
	γ-benzo[*b*]thiophene	3.283 ± 0.036	160.1 ± 1.5	3.669 ± 0.017	157.9 ± 3.9	170.0 ± 7.7
	Aromatic ring	3.160 ± 0.013	165.3 ± 1.1	-	-	-
	Alkyl chain	3.250 ± 0.015	160.7 ± 1.6	-	-	-
Thiourea	β-benzo[*b*]thiophene	3.240 ± 0.040	162.1 ± 1.2	3.706 ± 0.010	151.8 ± 4.7	158.9 ± 4.0
	γ-benzo[*b*]thiophene	3.204 ± 0.008	162.8 ± 0.3	3.812 ± 0.013	137.5 ± 0.4	135.0 ± 2.9
	Alkyl chain	3.216 ± 0.021	161.6 ± 1.9	-	-	-

[a] See Tables S1 and S2 for complete data and for ranges, respectively.

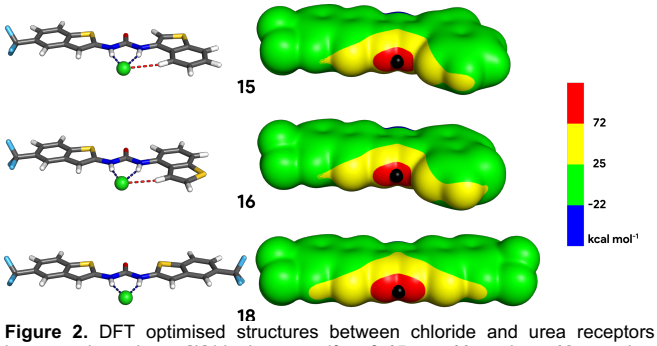

Figure 2. DFT optimised structures between chloride and urea receptors incorporating α-benzo[*b*]thiophene motifs α,β-**15**, α,γ-**16**, and α,α-**18**, together with the V_S of the corresponding receptors. Remaining details as given in Figure 1.

The dimensions of the N-H···Cl$^-$ and C-H···Cl$^-$ hydrogen bonds are gathered in Table S1, considering the (thio)urea decorating motifs, *i.e.*, the α-, β- and γ-benzo[*b*]thiophenes and aryl or alkyl substituents. Further clustering of data by urea and thiourea central binding units allowed us to calculate the average geometric parameters for both conventional and unconventional hydrogen bonding contacts by (thio)urea decorating fragments, as listed in Table 2. Although the fluorination of the α-benzo[*b*]thiophenes (**17** and **14** *versus* **15**, **16** and **18**) or aryl moieties (**20** *versus* **19**, **21**, **22**, **23** and **24**) naturally afforded stronger hydrogen bonding interactions with slightly shorter N···Cl$^-$ distances, grouping them with the non-fluorinated ones still yielded average values with low standard deviations. In the urea-based complexes, the N···Cl$^-$ distances for N-H groups linked to α-benzo[*b*]thiophene motifs are *ca.* 0.1 Å shorter than for N-H groups contiguous to β- and γ-benzo[*b*]thiophenes or alkyl chains, as a result from the polarisation of the adjacent $C_\alpha^{\delta+}$-$S^{\delta-}$ bond, in agreement with V_s distribution of the isolated benzo[*b*]thiophene[6] Of note, the N_α···Cl$^-$ distances, regardless of the fluorination of the α-benzo[*b*]thiophene ring (**14**-**18**), are identical to those where the N-H units are attached to aryl moieties decorated with an ester alkyl chain (**20**-**23**) or activated by two electron-withdrawing -CF_3 substituents (**19** and **24**). The thiourea chloride complexes display N-H···Cl$^-$ hydrogen bonds with comparable N···Cl$^-$ distances, regardless of the β- and γ-benzo[*b*]thiophenes (**12** and **10**) or aliphatic decorating motifs (**2**, **4**, **6** and **8**).

The average C···Cl$^-$ distances ascertained from both urea and thiourea-based receptors, ranging from 3.690 to 3.820 Å, are consistent with the existence of non-classical hydrogen bonds between the β- or γ-benzo[*b*]thiophene moieties and chloride. However, while all urea benzo[*b*]thiophene complexes display C-H···Cl$^-$ angles of *ca.* 160°, akin to the N-H···Cl$^-$ angles observed for the classical hydrogen bonds, in the thiourea anion complexes the C-H···Cl$^-$ angles for β- and γ-benzo[*b*]thiophene moieties are markedly different. Thus, the chloride complexes of β-benzo[*b*]thiophene derivatives **2**, **4** and **10** have C-H···Cl$^-$ angles of 158, 155 and 147°, respectively, while the γ-benzo[*b*]thiophene analogues (**6**, **8** and **12**) exhibit more acute C-H···Cl angles of *ca.* 138°.

The twisting of benzo[*b*]thiophene binding motifs was measured using the torsion angle ξ at the $C_\alpha/C_\beta/C_\gamma$-N central bond between the urea binding unit and the heteroaromatic fragment, as defined in Scheme 3. The values obtained for the twenty-four optimised geometries (see Table S1) were also cluster analysed and are listed in Table 2. The α- and β-benzo[*b*]thiophene fragments and the central urea binding unit are coplanar, as illustrated by the chloride complexes of β,β-**9**, α,β-**15** and α,α-**18** bis-benzo[*b*]thiophene derivatives, with ξ angles of 180° for both decorating motifs. In contrast, the lower average ξ angle, with a larger standard deviation (170.0° ± 7.7), obtained for the γ-benzo[*b*]thiophene fragment suggests that this heterocyclic ring tends to be more twisted when compared to the urea binding group, adopting a wider range of ξ angles, from 180° for the α,γ-**16** derivative, to 165.1° for the β,γ-**13**, and to 160.2° for the γ,γ-**11** bis-benzo[*b*]thiophene. On the other hand, in the thiourea β- and γ-benzo[*b*]thiophene-based complexes, to minimise the steric hindrance between sulfur and the C_α-H (thiophene) or C_δ-H (benzene) protons, the thiourea binding units are significantly twisted compared to the benzo[*b*]thiophene motifs, leading to even acuter average ξ angles, ranging from 155.1° in the β,β-**10** to 164.8° in the β,butyl-**2** derivatives and from 132° in the γ,γ-**12** to 138.2° in the γ,hexyl-**8** derivatives. Of note, the experimental chloride binding affinity of the symmetrical bis-benzo[*b*]thiophene-based receptors (Table 1), following the sequence β,β-**9** > γ,γ-**11**> β,β-**10** > γ,γ-**12**, appears to decrease as these ligands deviate from planarity (average ξ angles lower than 180°), leading to a linear relationship between the ξ parameter and log(K_a) values, with an R^2 of 0.92 (see Figure 3). Indeed, the γ,γ-**12** derivative displays the highest twisting degree with ξ angles of 138.2° with the two C_β-H protons at longer distances from chloride (2.9 Å), precluding anion recognition in a cooperative fashion with the N-H binding units, hence this receptor has the lowest binding constant within this subset. For the remaining complexes,

straightforward relationships between the structural parameters measured in their optimised geometries and the experimental binding constants were not apparent and required a more thorough evaluation of the strength the N-H···Cl$^-$ and C-H···Cl$^-$ hydrogen bonds using energetic binding descriptors calculated from the optimised structures of the twenty-four chloride complexes as follows.

The anion binding ability of a synthetic receptor is often related to the acidic character of its binding sites[10] and can be theoretically assessed by mapping the most positive value of the electrostatic potential ($V_{S,max}$) onto the receptor's electron density surface (V_S). The V_S of each receptor was calculated using its geometry in the optimised chloride complex. The V_S, including the location of $V_{S,max}$, is depicted in Figure 1 andFigure **2** for the β,β- (**9** and **10**), γ,γ- (**11** and **12**) and fluorinated α- (**15**, **16** and **18**) benzo[*b*]thiophene-based ureas, respectively, and in Figures S53 and S54 for the remaining molecules in the library. The $V_{S,max}$ values are given in Table 1 together with the experimental binding constants. As excepted, the most positive region of V_S encloses both (thio)urea N-H binding sites, with the $V_{S,max}$ located in front of them. The aliphatic benzo[*b*]thiophene ureas (**1**, **3**, **5** and **7**) display equivalent $V_{S,max}$ values (*ca.* 74 kcal mol^{-1}), while the corresponding benzo[*b*]thiophene thioureas (**2**, **4**, **6** and **8**) have $V_{S,max}$ values of *ca.* 79 kcal mol^{-1}. In other words, the thiourea protons are the most acidic in the aliphatic subset of receptors, although their higher acidity is not mirrored by higher binding constants when compared to the corresponding urea derivatives. In contrast, the β,β- (**9** and **10**), and γ,γ- (**11** and **12**) bis-benzo[*b*]thiophene (thio)urea derivatives exhibit comparable $V_{S,max}$ values, between 83 and 86 kcal mol^{-1}, for the γ,γ-**12** and β,β-**10** thioureas, respectively. Moreover, the β,γ-**13** asymmetric urea also has a $V_{S,max}$ within this narrow range.

Therefore, the superior binding affinity displayed by these three isomeric ureas for chloride is not dictated by their V_S. This finding is corroborated by the α,β-**14** isomer with a $V_{S,max}$ *ca.* 5 kcal mol^{-1} higher than the previous subset of receptors, due to the electron-withdrawing ability of the heterocyclic sulfur closer to N-H binding unit, which has a smaller chloride affinity of 125 M^{-1}. This counterintuitive trend proceeds with the α,α-derivative **17**, which has a binding constant of only 54 M^{-1} and a $V_{S,max}$ of 93 kcal mol^{-1} as a result of the two N-H protons being equally activated by two α-benzo[*b*]thiophene motifs. On other hand, the fluorination of **17** with two electron-withdrawing -CF_3 substituents affords the receptor with most acidic character in this library, α,α-benzo[*b*]thiophene **18**, with a $V_{S,max}$ of 102 kcal mol^{-1} and a slightly higher binding affinity of 86 M^{-1}. The fluorination of α,β-**14**, resulting in **15**, also leads to an increase of $V_{S,max}$ (*ca.* 5 kcal mol^{-1}) and a concomitant increase in the corresponding binding constant to 180 M^{-1}. Strikingly, the α,γ-**16** and α,β-**15** fluorinated isomers have similar $V_{S,max}$ values and experimental chloride binding affinities.

The increasing degree of fluorination in the aryl substituted subset of receptors naturally leads to an increase in $V_{S,max}$, with the molecules with two -CF_3 substituents directly attached to the phenyl ring (β- and γ-benzo[*b*]thiophene derivatives **19** and **24**, respectively) having $V_{S,max}$ values equivalent to the β-benzo[*b*]thiophene **23**, with a single aromatic -CF_3 substituent and a highly fluorinated ester alkyl chain (see Table 1). Moreover, $V_{S,max}$ increases with the insertion of a -CF_3 substituent in the aryl ring of β-benzo[*b*]thiophene **20**, yielding **21**, and subsequently with the progressive fluorination of its ester alkyl chain (affording **22** and **23**), with $V_{S,max}$ ranging from 88 (**20**) to 95 kcal mol^{-1} (**23**). However, the progressive growth of the acidic character of the urea binding unit along the **20**-**23** receptors is not accompanied by their experimental binding affinities for chloride, with **22**, with an intermediate $V_{S,max}$ value of 93 kcal mol^{-1}, having the highest chloride association constant of the whole library. On the other hand, **19** and **24** display similar $V_{S,max}$ values (*ca*. 95 kcal mol^{-1}), with the former, a β-benzo[*b*]thiophene derivative, presenting a slightly higher affinity constant, following the experimental binding trend observed between β,β- and γ,γ-benzo[*b*]thiophene-based ureas **9** and **11**, respectively.

The quantum descriptor $V_{S,max}$ only allowed us to rationalise the chloride binding affinity between non-fluorinated and fluorinated bis-benzo[*b*]thiophene analogues, given that, in this comprehensive library of small-molecules, this property is not solely dictated by the acidic character of the (thio)urea binding unit. This fact prompted us to evaluate the strength of the N-H···Cl$^-$ and C-H···Cl$^-$ hydrogen bonds via the Natural Bond Orbital (NBO) approach, with estimates of their Second Order Perturbation energies (E^2), and the Quantum Theory of Atoms in Molecules (QTAIM) analyses, with the prediction of the energy of hydrogen bonds (E_{HB}) directly obtained from the potential energy density $\mathcal{V}$, as E_{HB} = ½$\mathcal{V}$ (see ESI for more details). The interaction energies, defined as $\Delta E = E_{complex} - E_{receptor} - E_{anion}$,[11] are also collected in Table 1 and S5.

The E^2 and E_{HB} values for the whole library of chloride complexes are reported in Table S3. Notably, the scatter plot of E^2 versus E_{HB} values, for both the N-H···Cl$^-$ and C-H···Cl$^-$ hydrogen bonds, follows a linear relationship (see Figure S55 with an R^2 value > 0.99), showing that these two quantum parameters are equivalent descriptors for these hydrogen bonding interactions. Henceforth, in the subsequent discussion, only the E_{HB} values will be used. Like the structural analysis of the hydrogen bonds, the E_{HB} values were also clustered in agreement with the decorating fragments attached to the urea or thiourea binding units, leading to the average values listed in Table 3.

Table 3. Average E_{HB} and E^2 values (kcal mol^{-1}) assessed for the single N-H···Cl$^-$ and C-H···Cl$^-$ interactions in the chloride complexes of twenty-four benzo[*b*]thiophene-based receptors, grouped by binding unit (urea or thiourea) and by its decorating motif.[a]

Binding unit	Decorating motif	N-H···Cl$^-$		C-H···Cl$^-$	
		E_{HB}	E^2	E_{HB}	E^2
Urea	α-benzo[*b*]thiophene	-6.7 ± 0.4	19.4 ± 1.4	-	-
	β-benzo[*b*]thiophene	-4.9 ± 0.3	13.8 ± 0.8	-1.5 ± 0.1	2.3 ± 0.3
	γ-benzo[*b*]thiophene	-4.4 ± 0.6	12.1 ± 1.9	-1.9 ± 0.0	3.4 ± 0.2
	Aromatic ring	-6.9 ± 0.4	20.8 ± 1.3	-	-
	Alkyl chain	-4.8 ± 0.3	12.3 ± 1.1	-	-
Thiourea	β-benzo[*b*]thiophene	-5.3 ± 0.8	15.4 ± 2.5	-1.6 ± 0.1	2.2 ± 0.4
	γ-benzo[*b*]thiophene	-5.9 ± 0.2	17.5 ± 0.3	-1.0 ± 0.0	1.0 ± 0.0
	Alkyl chain	-5.5 ± 0.5	15.1 ± 1.7	-	-

[a] See Tables S3 and S4 for complete data and for ranges, respectively.

Akin to the pattern of the N···Cl$^-$ distances for the hydrogen bonds, the E_{HB} values for the urea N-H units adjacent to the heterocyclic moieties follow the order α- (-6.7 kcal mol^{-1}) < β- (-4.9 kcal mol^{-1}) < γ-benzo[*b*]thiophenes (-4.4 kcal mol^{-1}), showing that a N-H binding unit activated by a vicinal thiophene sulphur increases the strength of the corresponding N-H···Cl$^-$ hydrogen bond. On the other hand, the chloride complexes of two α,α-benzo[*b*]thiophenes, with E_{HB} values for both N-H binding units of -12.6 (**17**) and -13.0 (**18**) kcal mol^{-1}, have the lowest experimental binding constants among the complexes of bis-benzo[*b*]thiophenes derivatives (54 and 86 M^{-1}, respectively), regardless of the greater acidic character of **18** (*vide supra*) provided by the two electron-withdrawing -CF_3 substituents. The linkage of a β- or γ-benzo[*b*]thiophene in the place of a α-benzo[*b*]thiophene yields asymmetrical receptors with improved experimental binding affinities of 125 (α,β-, **14**), 180 (α,β-, **15**), and 179 M^{-1} (α,γ-, **16**). Paradoxically, the E_{HB} values estimated for the two convergent N-H···Cl$^-$ hydrogen bonds in these three chloride complexes are *ca.* -11.8 kcal mol^{-1}, indicating that these bonding interactions are weaker when compared to those for complexes of α,α-benzo[*b*]thiophenes **17** and **18**. Therefore, the higher binding ability of the α,β- and α,γ-benzo[*b*]thiophene-based ureas, in agreement with the optimised structures of their chloride complexes, results from the single C-H···Cl$^-$ bonding interaction with a E_{HB} energy of *ca.* -1.4 and -1.8 kcal mol^{-1} for the C_γ-H and C_β-H binding sites, respectively in the α,β- and α,γ-benzo[*b*]thiophene derivatives. In the chloride complexes of γ,γ- and β,γ-benzo[*b*]thiophene ureas, with association constants of 209 (**11**) and 199 M^{-1} (**13**), the two synergetic C-H···Cl$^-$ interactions amount to an E_{HB} energy of -3.7 kcal mol^{-1}, while the contribution of both N-H binding sites to the E_{HB} energy is *ca.* -10.2 kcal mol^{-1}. The complex for the β,β-benzo[*b*]thiophene receptor **9**, with a slightly higher association constant (254 M^{-1}), has two convergent N-H···Cl$^-$ hydrogen bonds assisted by two C-H···Cl$^-$ bonding contacts with E_{HB} energies of -10.5 and -3.3 kcal mol^{-1}, respectively. The lower chloride binding constants measured for the thiourea analogues of the symmetrical ureas, 124 M^{-1} (β,β-, **10**) and 56M^{-1} (γ,γ-, **12**), reflect the different strength of the C-H···Cl$^-$ interactions with E_{HB} energies of -3.1 and -2.1 kcal mol^{-1} respectively, as the classical hydrogen bonds contribute an equal amount of E_{HB} energy (*ca.* -12.0 kcal mol^{-1}) for the stabilisation of both complexes. Furthermore, while the values of E_{HB} energies of the C-H···Cl$^-$ interactions indicate that they are weaker in the **12** γ,γ-benzo[*b*]thiophene thiourea complex than in its **11** urea analogue, the E_{HB} energy differences of these ancillary interactions in the chloride complexes of β,β-benzo[*b*]thiophenes **9** and **10** are not meaningful, suggesting that other structural features contribute to the stabilisation of this subset of bis-benzo[*b*]thiophene complexes. The interaction energies (see Table S5) linearly decrease with an increase in the logarithm of the association constant, log(K_a), across the subset of bis-benzo[*b*]thiophenes **9-12**, with a R^2 of 0.86, following the reverse trend found for the ξ twisting parameter (see Figure 3). Overall, these insights indicate that, in the chloride complex of the β,β-derivative **10**, the putative steric clashes between the negatively charged thiourea sulfur and the most positively charged C_α-H protons from two thiophene rings (see Scheme 3) are related to the twisting of both benzo[*b*]thiophene rings relative to the thiourea binding unit, while the C-H···Cl$^-$ binding interactions are equivalent to those observed in the **9** β,β-urea-analogue. In contrast, the relaxed structure of the **12** γ,γ-complex is only achieved with a stronger distortion from the planarity of both γ-benzothiophene moieties, with concomitant weakening of the C_β-H···Cl$^-$ interactions when compared with the more planar **11** β,β-urea analogue (*vide supra*).

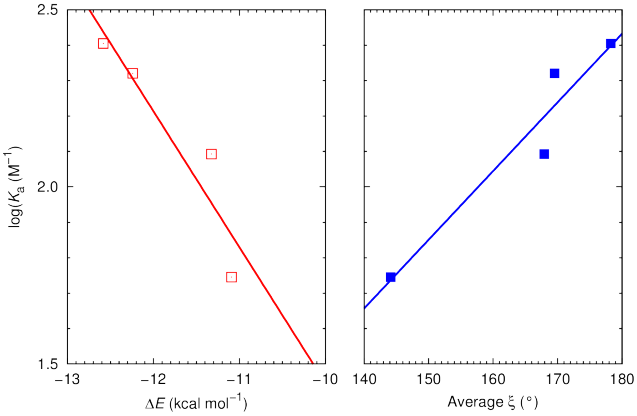

Figure 3. Log(K_a) plotted against ΔE (□, left) and against the average value of the ξ twisting angle (■, right) for the chloride complexes' subset of β,β- (**9** and **10**), and γ,γ- (**11** and **12**) bis-benzo[*b*]thiophene (thio)urea derivatives. The corresponding linear regressions have R^2 = 0.86 (red line) and R^2 = 0.92 (blue line).

According to the E_{HB} energies for the N-H···Cl$^-$ (see Table 3) interactions, the values become slightly more negative with fluorination of the α-benzo[*b*]thiophene motifs (α,α-**17** *versus* α,α-**18** and α,β-**14** *versus* α,β-**15**) following the increasing binding constants values.

Unfortunately, this detailed analysis cannot be applied to the aliphatic or aromatic derivatives. The small magnitude and similarity between the association constants for the aliphatic β- or γ-benzo[*b*]thiophene-based receptors, **1**-**8**, does not allow us to determine a relationship with the quantum descriptors at hand.

Also, the structural similarities found for the optimised structures of the chloride complexes of aryl derivatives **19**-**24** leads to quantum descriptors with low variability and subsequent difficulties relating them with broader experimental binding constants. Overall, the chloride binding association constants and quantum descriptors found for the bis-benzo[*b*]thiophenes **9**-**18** are most likely a consequence of the geometrical constrains inherent to their ability as anion binders.

Crystallographic studies Suitable single crystals for X-ray structure determination of eight urea benzo[*b*]thiophene-based molecules were grown from the final DMSO solutions obtained from the titrations of the receptors with TBACl. Even with an excess of chloride in solution, only complexes of **9**, **14**, **15** and **21** were obtained, with the remaining mono-urea derivatives crystalising as free receptors (**5**, **11** and **22**) or hydrogen bonded to a single competitive DMSO solvent molecule (**16**, **19**, **20** and **24**).

The free receptors display non-planar conformations with the γ-benzo[*b*]thiophene moieties twisted relative to the central urea binding unit, as shown by the perspective views of their asymmetric units presented in Figure 4. In line, the γ- and β-benzo[*b*]thiophene derivatives **5** and **22** have ξ angles (*vide supra*) of -140.5(2)° and 146.7(2)°, respectively, while in **11**, the ξ angles for the two γ-benzo[*b*]thiophene units are 63.4(2)°, indicating a higher degree of twisting. These distinct values are the result of the self-assembly of these three small molecules into one-dimensional chains through convergent hydrogen bonds between carbonyl groups and urea binding units of adjacent molecules (Figures S56 to S58).

In contrast, the recognition of DMSO by the aryl γ-benzo[*b*]thiophene **24** and aryl β-benzo[*b*]thiophene derivatives **19** and **20** leads to ξ values close to 180° (Scheme 3), leaving these heteroaromatic moieties nearly coplanar with the binding unit. On the other hand, **16** displays two distinct ξ parameters of -168.3(2) and 179.7° for the β- and α-benzo[*b*]thiophene moieties, respectively. Furthermore, the perspective views of these complexes, presented in Figure 5, show that both C_{γ}-H protons of **19** and **20** and the C_{β}-H protons of **24** and **16** point towards the DMSO oxygen atom, which enables the formation of C-H···O=S bonding contacts, as observed for the **16**·DMSO association with a C···O distance of 3.437(3) Å and C-H···O angle of 156°.

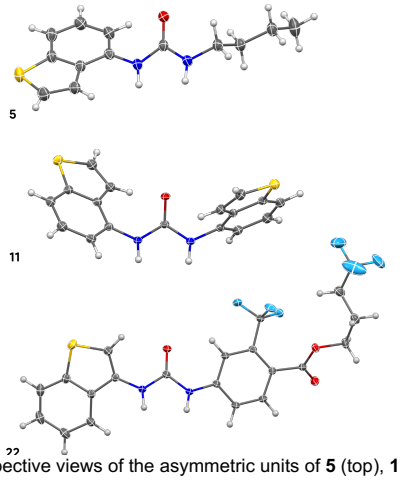

Figure 4. Perspective views of the asymmetric units of **5** (top), **11** (centre), and **22** (bottom) with thermal ellipsoids drawn at the 40% probability level.

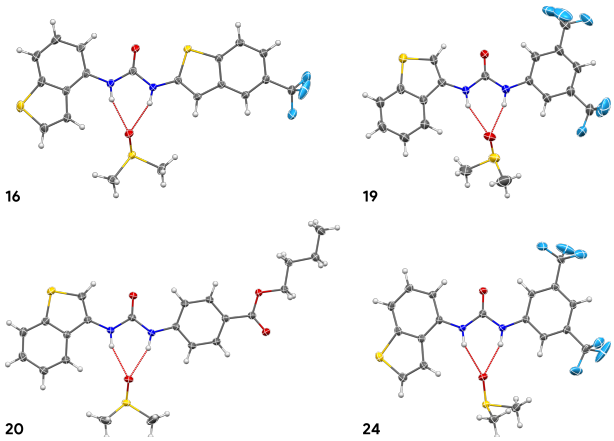

Figure 5. Perspective views of the DMSO associations of **16**, **19** (molecule B), **20**, and **24**, with thermal ellipsoids drawn at the 40% probability level. The N-H···O hydrogen bonds are drawn as red dashed lines.

The dimensions of the two convergent hydrogen bonds between DMSO and **16**, **19**, **20**, and **24** are gathered in Table 4. In the isomeric ureas **19** and **24**, the DMSO hydrogen bond to the N-H adjacent to aryl moiety is stronger, with a N_{arom}···O distance which is slightly shorter than the N_{β}/N_{γ}···O distances. This structural feature is due to the presence of two -CF_3 electron withdrawing groups in the aryl substituents and is also observed in the DMSO complex of the α,γ-benzo[*b*]thiophene derivative **16**, with N_{γ}···O and N_{α}···O distances of 2.865(2) and 2.803(2) Å. Indeed, the latter distance is the shortest seen in the fluorinated receptors, which results from this compound having the highest acidic character for the N-H binding site near the -CF_3 substituted α-benzo[*b*]thiophene. The calculated electrostatic potential distribution for **16** backs this observation up (*vide supra*).

Table 4. Values of the hydrogen bond dimensions[a] found in the with DMSO or Cl^- complexes, together with the ξ angles of the receptors.

Complexes	Proton donor	N···X[b]	∠ N-H···X[b]	∠ ξ	Proton donor	N···X[b]	∠ N-H···X[b]	∠ ξ
20·DMSO	N_{β}	2.906(2)	156	171.1(1)	N_{arom}	2.877(2)	159	-
24·DMSO	N_{γ}	2.878(3)	156	175.7(2)	N_{arom}	2.829(3)	158	-
16·DMSO	N_{β}	2.865(2)	155	-168.3(2)	N_{α}	2.803(2)	158	179.7(2)
19·DMSO[c]								
A	N_{β}	2.903(7)	153	-179.7(5)	N_{arom}	2.850(7)	145	-
B	N_{β}	2.934(6)	153	-175.4(4)	N_{arom}	2.812(6)	162	-
9·Cl^-	N_{β}	3.205(2)	159	163.7(2)	N_{β}	3.206(2)	155	177.6(2)
14·Cl^-	N_{β}	3.243(2)	156	176.9(2)	N_{α}	3.185(2)	160	-180.0(2)

15$_2$·Cl$^-$								
A	N_β	3.306(2)	156	-156.9(2)	N_α	3.169(2)	162	-177.0(3)
B	N_β	3.340(2)	153	177.5(2)	N_α	3.214(2)	148	176.3(2)
21·Cl$^-$	N_β	3.305(3)	156	-169.4(3)	N_{arom}	3.136(3)	168	-

[a] All distances are in Å and angles in °; [b] X = O or Cl$^-$; and [c] The asymmetric unit of **19**·DMSO is composed of two molecules of **19** and two molecules of DMSO.

The β-benzo[*b*]thiophene-based ureas, **9**, **14** and **21**, bind a chloride anion through two synergetic N-H···Cl$^-$ hydrogen bonds resulting in a short distance between the C_γ-H protons and the anion, (see Figure 6). However, while the N···Cl distances listed in Table 4, show that these interactions have equivalent strengths in the symmetrical β,β-benzo[*b*]thiophene chloride complex **9**, in the asymmetrical complex **21**, the N_{arom}···Cl distance is *ca*. 0.2 Å shorter than N_β···Cl distance that results from the electron-withdrawing character of the fluorinated ester decorating motif. In the asymmetrical α,β-benzo[*b*]thiophene complex **14**, the N-H···Cl$^-$ hydrogen bonds display different strengths, with N_α···Cl$^-$ and N_β···Cl$^-$ distances of 3.185(2) and 3.243(2) Å, respectively. This slight difference corroborates the higher acidic character predicted for the urea binding unit directly bonded to an α-benzo[*b*]thiophene fragment. Tetrabutylammonium cations shelter these three chloride complexes and prevent the formation of species with a stoichiometry superior to 1:1 in the solid-state. In contrast, the complex between the α,β-benzo[*b*]thiophene derivative **15** and chloride exhibits a 2:1 stoichiometry with the anion hydrogen bonded by two molecules (A and B), as shown in Figure 6. The ligands A and B are tilted with respect to each other, by a dihedral angle of 56.1° between their average planes. Moreover, while B adopts a planar conformation with two ξ parameters near 180° (Table 4), A is more distorted with ξ angles of -156.8(2) and 177.0(3)°, respectively. The DMSO association with the α,γ-benzo[*b*]thiophene isomer **16** has N···Cl distances (Table 4) that suggest that the two hydrogen bonds to the N_α-H binding units are stronger than those involving the N_β-H binding units.

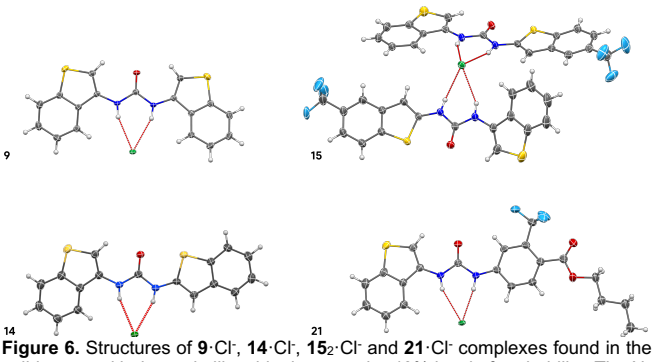

Figure 6. Structures of **9**·Cl$^-$, **14**·Cl$^-$, **15**$_2$·Cl$^-$ and **21**·Cl$^-$ complexes found in the solid-state, with thermal ellipsoids drawn at the 40% level of probability. The N-H···Cl- hydrogen bonds are drawn as red dashed lines.

Efflux studies The anion transport activity of the mono-(thio)urea-based transporters was initially assessed using the chloride-nitrate exchange assay. Large unilamellar vesicles (LUVs, 200 nm) prepared from POPC were loaded with a NaCl internal solution (487 mM, pH 7.20). The vesicles were suspended in a $NaNO_3$ external solution (487 mM, pH 7.20). The transporters were added as a DMSO solution (10 μL), and the rate of chloride efflux into the external solution was measured using a chloride selective electrode (ISE). Concentration dependent studies were performed, followed by Hill analysis of the chloride efflux at 270 s to determine the effective concentration for the transporters to facilitate 50% efflux (EC_{50}, Table 1 and Figures S59-S68). The assay demonstrated a Cl$^-$/NO_3^- exchange activity of the following: **19** > **15** > **24** > **10** > **13** > **22** > **16** > **23** > **21**, with the β-benzo[*b*]thiophene-based urea **19** showing the highest potency (EC_{50} = 0.4240). Initial rates of chloride efflux (Table 1) attained through the same assay followed parallel trends to the concentration-dependent investigation. The non-fluorinated vastly underperformed compared to the fluorinated transporters, suggesting that lipophilicity and increased hydrogen bond acidity are valuable characteristics for increasing transport activity. The chloride-nitrate exchange assay is typically a fair assessment for evaluating chloride transport activity. However, it was ineffective in obtaining EC_{50} values for a large portion of this benzo[*b*]thiophene-based library. A possibility of this inconsistency may lie with the compounds' ability to bind and transport NO_3^-, as chloride transport is no longer the rate limiting step, the activity may prove to be an underestimation of chloride transport capability.[12]

Investigations into the chloride transport mechanism facilitated by the thiophene-decorated anionophores were then performed using cationophore-coupled assays (Figure 7a). KCl (300 mM, pH 7.20) solutions were loaded into POPC LUVs (200 nm) suspended in KGlu (300 mM, pH 7.20). The transporters were added as a DMSO solution (10 μL), and valinomycin (an electrogenic K^+ uniporter) or monensin (an electroneutral M^+/H^+ cotransporter) were added to induce chloride efflux measured by ISE. Chloride efflux in the presence of both valinomycin and monensin was observed in all instances. Electrogenic chloride transport was shown to be more efficient over electroneutral transport for most of the library, apart from compounds **14**, **18** and **20** which showed an equivalent affinity to both transport mechanisms (Figure 7b, S69 and S70).

Further elucidation of transport ability and Cl^- > H^+/OH^- selectivity of the receptors was achieved using a modified *N*-methyl-D-glucamine chloride (NMDG-Cl) assay.[13] 8-Hydroxypyrene-1,3,6-trisulfonic acid (HPTS, a pH sensitive dye) and NMDG-Cl (100 mM, pH 7.0) were loaded into POPC LUVs (200 nm) and suspended in an external solution of NMDG-Cl (100 mM, pH 7.0). The transporters were added as a DMSO solution (5 μL), and a NMDG base pulse was added to initiate chloride efflux. Each receptor was subjected to three separate conditions (Figure 7c): a) Oleic acid (OA, 2 mol%) was used to examine the Cl^-/H^+ cotransport through fatty acid flip-flop, a naturally occurring proton shuttling pathway; b) Bovine serum albumin (BSA, 1 mol%) was employed to treat vesicles, sequestering fatty acids and diminishing Cl^-/H^+ cotransport through fatty acid flip-flop; and c) Gramicidin (Gra, 0.1 mol%) to facilitate electrogenic H^+ efflux to assess Cl^- uniport. Concentration-dependent Hill analyses allowed the calculation of EC_{50} values (see Figures S71-S106) summarised in Table 5. The selectivity of Cl^- uniport over H^+/Cl^- symport was quantified through the ratio of the $EC_{50\,(BSA)}$ treated and $EC_{50\,(Gra)}$ values, generating a chloride selectivity factor (F_{Gra}) (Table 2). All compounds showed an enhancement in chloride transport (F_{Gra} values >1) indicating universal Cl^- > H^+/OH^- selectivity, **13** showed the largest enhancement supporting findings from the cationophore-coupled assay. Evaluations of the

transporter's capability to contribute to fatty acid flip-flop were assessed through the ratio of the $EC_{50\ (BSA)}$ treated and $EC_{50\ (OA)}$ values to afford F_{OA} (Table 5). Increased chloride transport was observed for all compounds across the series upon addition of OA (F_{OA} values >1), indicating that the rate of H^+/Cl^- symport increased due to transporter mediated fatty acid flip-flop. Assessment of the compounds ability to retain chloride selective transport in the presence of OA ($F_{OA/Gra}$) was attained through the ratio of the $EC_{50\ (OA)}$ and $EC_{50\ (Gra)}$ values (Table 5). Minor amounts of retention were seen across the series ($F_{Gra/OA}$ > 1), with compound **13** showing the highest chloride selective transport. Whereas compounds **16** and **18** showed no chloride selective retention ($F_{Gra/OA}$ < 1). In conjunction with the cationophore-coupled assay, the results signify that Cl^- uniport is the favoured transport mechanism for the thiophene-based transporters.

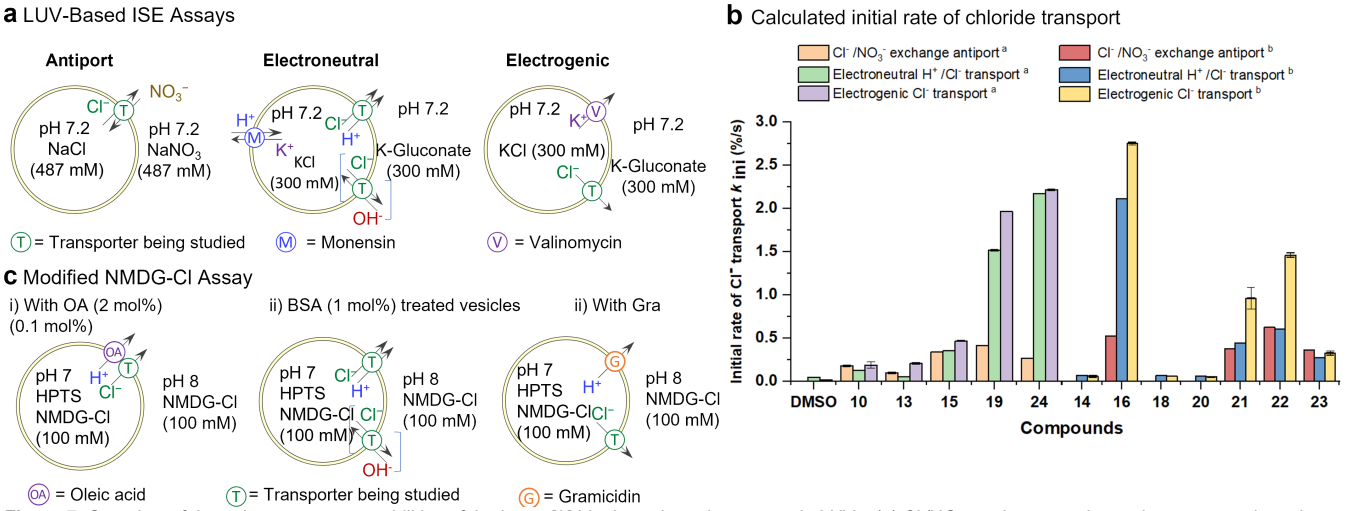

Figure 7. Overview of the anion transport capabilities of the benzo[*b*]thiophene-based receptors in LUVs. (a) Cl^-/NO_3^- exchange and complementary cationophore-coupled assays used to determine transport mechanisms. Where T = transporter, M = monensin and V = valinomycin; (b) Initial rates of chloride transport calculated by exponential or linear fitting for each transporter a) (1 mol%), and b) (20 mol%) under various conditions; (c) The three different conditions utilised during the *N*-methyl-D-glucamine chloride (NMDG-Cl) assay, monitored by 8-hydroxypyrene-1,3,6-trisulfonic acid (HPTS) fluorescence: i) the addition of oleic acid (OA) (2 mol%), ii) pre-treatment of BSA (1 mol%), and iii) the addition of gramicidin (0.1 mol%).

Table 5. EC_{50} values shown for the NMDG-Cl assay with benzo[*b*]thiophene-based receptors in BSA treated vesicles, in the presence of gramicidin (Gra) and in the presence of oleic acid (OA).

Compound	NMDG-Cl Assay EC_{50} (mol%)[a]			Selectivity		
	With OA	With Gra	BSA treated	F_{Gra}[b]	F_{OA}[c]	$F_{Gra/OA}$[d]
β,β-benzo[*b*]thiophenes						
10	0.95756	0.77103	2.55325	3.3	2.7	1.2
β,γ-benzo[*b*]thiophene						
13	1.17056	0.57659	5.91853	10.3	5.1	2.0
α,β-benzo[*b*]thiophenes						
14	0.07730	0.06340	0.18510	2.9	2.4	1.2
15	0.19335	0.19341	0.34814	1.8	1.8	1.0
α,γ-benzo[*b*]thiophenes						
16	0.01300	0.01550	0.07630	4.9	5.9	0.8
α,α-benzo[*b*]thiophenes						
18	0.01940	0.02536	0.05260	2.1	2.7	0.8
Aryl β-benzo[*b*]thiophenes						
19	0.08995	0.07696	0.16685	2.2	1.9	1.2
20	0.06450	0.03930	0.31570	8.0	4.8	1.7
21	0.03300	0.02800	0.10230	3.7	3.1	1.2
22	0.02590	0.02140	0.05790	2.7	2.2	1.2
23	0.03290	0.03220	0.18430	5.7	5.6	1.0
Aryl γ-benzo[*b*]thiophene						
24	0.09527	0.09248	0.22988	2.5	2.4	1.0

[a] Values reported in transporter to lipid molar ratio (mol%); [b] Factor of enhancement in the Cl^- uniport in the presence of Gra, F_{Gra} is calculated by dividing the $EC_{50\ (BSA)}$ by the $EC_{50\ (Gra)}$. F_{Gra} > 1 indicates Cl^- transport enhancement; [c] Factor of enhancement in the overall rate of Cl^-/H^+ cotransport in the presence of OA, F_{OA} is calculated by dividing the $EC_{50(BSA)}$ by the $EC_{50(OA)}$. F_{OA} > 1 indicates the receptor can assist the flip-flop of OA, increasing pH dissipation. [d] Factor of Cl^- > H^+/OH^- selectivity retention in the presence of OA, $F_{Gra/OA}$ is calculated by dividing $EC_{50(Gra)}$ by $EC_{50(OA)}$; $F_{Gra/OA}$ > 1 indicates Cl^- selective retention in the presence of OA.

Molecular Dynamics simulations in POPC membrane model

Further insights into the transport ability of our library of benzo[*b*]thiophene (thio)urea-based molecules were obtained through Molecular Dynamics (MD) simulations undertaken with chloride complexes of **1**, **9**, **15**, **16**, **18**, **19**, **23** and **24**, embedded in a POPC bilayer membrane model. These eight complexes were selected based on their experimental efflux data, as well as their lipophilic character, binding ability, and the structural peculiarities of their receptors. The MD simulations were carried out using the AMBER 18 GPU-based simulation engine,[14] with classical force field parameters, as detailed in the ESI. Two alternative starting scenarios with each chloride complex initially placed in the aqueous phase (scenario *A*) or at the bilayer core (scenario *B*) were simulated along two independent MD runs of 200 ns. The passive diffusion of each small-molecule across the phospholipid bilayer was monitored by evaluating the relative distances along the *z* coordinate (water/lipid interface normal axis), between two reference points of the receptor: the centres of mass of each urea decorating motif (c_1 and c_2 defined in Scheme 4A and Scheme 4B); and the closest bilayer interface (P_{int}, defined by the average *z* coordinate of the phosphorus atoms in that leaflet). The evolution of these relative distances throughout the MD runs are plotted in Figures S107 to S110, together with the total number hydrogen bonding interactions between each receptor and chloride. In the passive diffusion MD simulations, the chloride surrounded by water molecules is released during the earlier stages of the MD runs, before the receptors permeate the water/lipid interface (scenario *A*). In the alternative scenario *B*, where the complexes are initially located within the bilayer, chloride release occurs as the complexes get closer to the water/lipid interface, with the event being assisted by water molecules from the water phase.

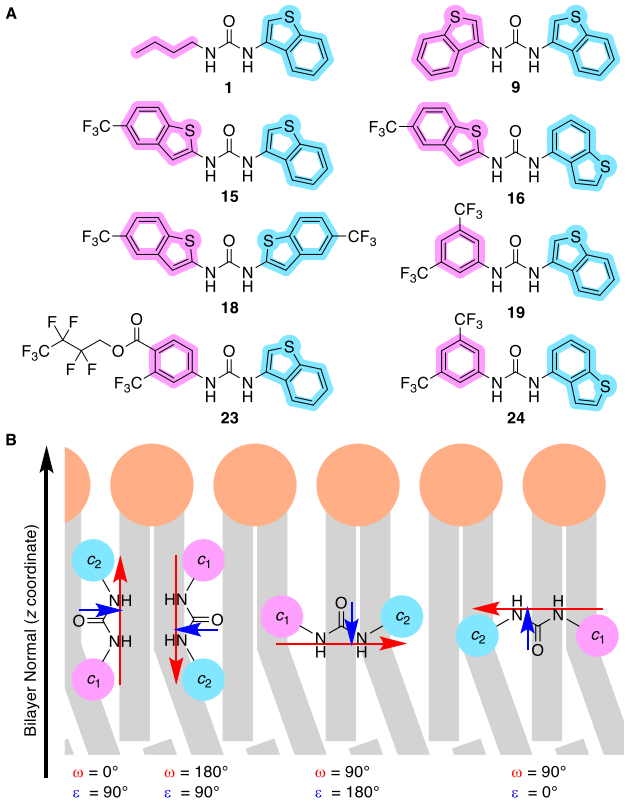

Scheme 4. (**A**) Sketches of **1**, **9**, **15**, **16**, **18**, **19**, **23** and **24**, with the atoms used to define the c_1 and c_2 centres of mass highlighted in pink and light blue. (**B**) Illustration of putative receptor orientations in the bilayer and corresponding ω and ε angles between the $\overrightarrow{c_1c_2}$ (red arrow) and $\overrightarrow{OC}$ (blue arrow) vectors and the bilayer normal (*z* coordinate).

For the majority of the simulation time, regardless of the starting scenario, the selected benzo[*b*]thiophene-based ureas are located below the water/lipid interface level, but, depending on their decorating motifs, acquire different orientations between the phospholipids, which were measured using the ω and ε angles defined in Scheme 4B. Angle ω is the angle between the vector defined by the two reference points in receptor ($\overrightarrow{c_1c_2}$, Scheme 4B) and the bilayer normal axis and gives the orientation of the whole molecule. Angle ε is the angle between the urea O=C bond ($\overrightarrow{OC}$) and the bilayer normal axis and gives the orientation of the urea binding unit with respect to the water/lipid interface. The ω and ε angles were evaluated throughout the simulation time for the four independent MD runs carried out for each receptor (see Figures S111 to S114). Overall, the variations observed in both angles are comparable, at least for the last 100 ns, for all simulations irrespective of MD run and starting scenario. Thus, the ω and ε angles calculated for the four runs for each receptor during this simulation period were concatenated, resulting in the average values and standard deviations given in Table 6.

The fluorinated fragments in **19** and **24** (the 3,5-bis-(trifluoromethyl) motifs) and in **15** and **16** (the 5-(trifluoromethyl)benzo[*b*]thiophene substituents) point to the bilayer core, while the β- or γ-benzo[*b*]thiophene moiety is closer to the water/lipid interface, resulting in ω angles between 62 and 72°, which indicates that these four asymmetric molecules adopt a tilted orientation relative to the bilayer normal axis. The symmetric receptors **9** and **18**, naturally display roughly parallel orientations relative to the water/lipid interface with the respective β,β- and α,α-benzo[*b*]thiophene rings at almost equivalent distances from the interface, resulting in ω values of around 81 and 91°. **23**, with an average ω angle of *ca*. 87°, has an equivalent orientation, with the fluorinated ester butyl chain embedded between the phospholipids. Furthermore, these seven receptors (**19**, **24**; **15**, **16**; **9**, **18**; and **23**) have average ε angles that range from 24 to 39°, indicating that their N-H urea binding sites point to the water/lipid interface, in line with the tilt of each receptor to the membrane reference (see Scheme 4).

The lipophilic imbalance in the decorating motifs of **1** give ω and ε angles of 89.4 ± 31.3° and 50.3 ± 34.1°, respectively. These average values, with their wide variations, suggest that this β-benzo[*b*]thiophene derivative with an aliphatic *n*-butyl chain, is not always pointing to the water phase and is tumbling between the phospholipids as shown by the plots in Figures S107 and S110. MD snapshots in Figure 8 and S115 illustrate the most common orientation observed for each small synthetic receptor.

Table 6. Average ω and ε angles (°), with their standard deviations, assessed for the cumulative sampling time in the MD runs of the different transporters.

Transporter	Angle ω	Angle ε
1	89.4 ± 31.3	50.3 ± 34.1
9	81.5 ± 24.7	31.4 ± 22.8
15	66.6 ± 19.3	29.1 ± 15.6
16	61.9 ± 22.1	39.3 ± 21.6
18	91.0 ± 19.0	24.0 ± 13.7
19	63.2 ± 19.4	34.7 ± 18.8
23	86.8 ± 20.8	28.4 ± 15.3

24	71.8 ± 24.8	37.6 ± 22.5

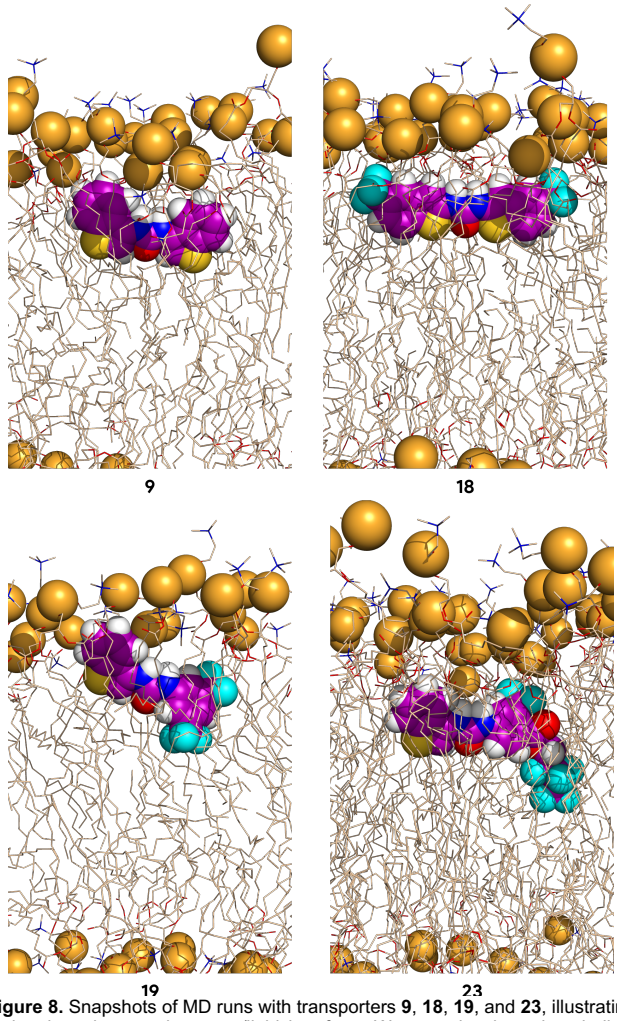

Figure 8. Snapshots of MD runs with transporters **9**, **18**, **19**, and **23**, illustrating their orientations at the water/lipid interface. Water molecules, phospholipid aliphatic protons, and ions were omitted for clarity.

The diffusion of the benzo[*b*]thiophene derivatives in the POPC bilayer is accompanied by hydrogen bonding interactions between the urea binding units and their surroundings. Figure S116 shows the average N-H interactions with chloride, water and phospholipid headgroups for the cumulative MD simulation time of each receptor (800 ns), along the bilayer normal axis. These small receptors establish up to two simultaneous hydrogen bonds, with the *sn*-1 and *sn*-2 ester groups being the least sought-after interactors. Apart from the typical exchange of interactions between water and the phosphate headgroups around z = 0 Å (varying to different extents, depending on the transporter), it is worth noting that these molecules are also able to recognise chloride in the water phase or close to the water/lipid interface – a vital step to promote chloride efflux across a bilayer.[6]

The understanding of the structural and energetic features associated with the anion transport promoted by **15**, **18** and **19** was obtained via Umbrella Sampling (US) MD simulations, followed by the estimate of the free energy (Potential of Mean Force, PMF) profiles associated with the translocation of these receptors, free or hydrogen bonded to chloride, using the variational free energy profile (vFEP) method.[15] Full computational details are given in the ESI. Figure 9 shows the PMF curves obtained with the free receptors as well as with their chloride complexes, when positionally restrained at different z coordinate values, varying between z = 0 Å (bilayer core) and z = 40 Å (bulk water) – to which all profiles were normalised (see Figure S117 for the PMF convergence). These energy profiles are also plotted in Figure S118 with the bootstrap errors calculated from 100 random data sets with the same size. The PMF minima and their positions are summarised in Table S9, together with the PMF values at z = 0 Å (bilayer core). The transition of the free receptors and their chloride complexes from the water phase to inside the bilayer is thermodynamically favoured, starting at z = 27 Å, with energy gains of *ca*. 1.5 kcal mol^{-1} for the free receptors when compared to their complexes. Moreover, the profiles for the chloride complexes reach a minimum around z = 10.7 Å while the minimum for the free molecules occurs 1.8 Å deeper in the bilayer at z = 8.9 Å. Undoubtedly, the solvation of the hydrogen bonded chloride is the main cause for these differences, leading to a minimum much closer to the water phase and with higher energy for the chloride complexes. Moreover, α,β-benzo[*b*]thiophene **15** is the compound with shallowest energy well, with minima of -5.3 (complex) and -6.5 kcal mol^{-1} (free), while **19** and **18** have almost overlapping energy profiles. Their chloride complexes have minima of -5.8 and -5.9 kcal mol^{-1}, while the corresponding free transporters have minima of -7.2 and -7.5 kcal mol^{-1}. At the bilayer core, to diffuse towards the opposite phospholipid leaflet, the chloride complexes must surmount an energy barrier of *ca*. 4.5 kcal mol^{-1}, while the free receptors face a 3.0 kcal mol^{-1} "climb". The energy barriers for **15** are slightly higher than for **19** and **18**, *ca*. 1.6 kcal mol^{-1}. Given the comparable energy profiles found for the fluorinated aryl,β-benzo[*b*]thiophene **19** and for bis-fluorinated α,α-benzo[*b*]thiophene **18**, the low transport ability of the latter appears to arise from its lack of an auxiliary C-H binding unit, which is mirrored in a smaller chloride association constant (*vide supra*).

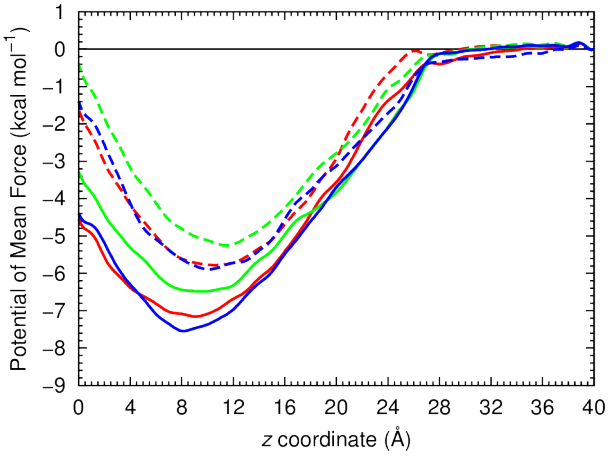

Figure 9. PMF as a function of transporters' distance to the membrane centre of mass (z = 0 Å), for free **15**, **18** and **19** (solid green, blue and red lines, respectively) and their Cl- complexes (dashed green, blue and red lines, in this order).

Orientation of **15**, **18** and **19** throughout the US windows was also evaluated using the ω and ε angles, which varies as shown in Figure S119, in agreement with the z coordinate position where the receptor or complex is being simulated. For z coordinate values between 0 and 12 Å, both ω and ε values are entirely consistent with observations on the passive diffusion MD simulations discussed above. However, as the free receptors are simulated closer to the water/lipid interface ($z \approx 18$ Å), wider

variations are observed in both angles, with the ω angle displaying the greater shifts. These variations can be ascribed to interactions with the phospholipid headgroups, as the chloride complexes (unable to interact with the membrane components), do not present such variations. At *z* coordinate values larger than 24 Å, both angles present average values of *ca*. 90° with standard deviations larger than 38°, as the receptors or chloride complexes are in bulk water and can freely reorient themselves.

Conclusion

In general, among the aliphatic β- and γ-benzo[*b*]thiophene-based receptor subset, the thiourea analogues display slightly higher affinities for chloride, reflecting the superior acidic character of the thiourea N-H binding groups compared to the N-H urea groups, as calculated from the $V_{S,max}$ quantum descriptor. In stark contrast, within the larger subset of the bis-benzo[*b*]thiophene-based molecules, the experimental binding constants of the β,β- and γ,γ-symmetrical thioureas (**10** and **12**) are significantly lower than those for their urea analogues (**9** and **11**), which is explained by the computed binding geometries obtained for the corresponding chloride complexes. The thiourea complexes display a higher degree of distortion, as measured by the ξ twisting parameter, leading to a weaker ancillary C-H···Cl^- hydrogen-bonding interaction, as also inferred from the E^2 and E_{HB} quantum descriptors. The relevance of these interactions for chloride binding affinity is also evident when the experimental binding data of the β,β-**9** and γ,γ-**11** bis-benzo[*b*]thiophenes are compared with their non-fluorinated β,γ-**13**, α,β-**14**, and α,α-**17** analogues. We find that **13**, able to establish two N-H···Cl^- and two C-H···Cl^- hydrogen-bonding interactions, has a binding affinity for chloride comparable to the γ,γ-receptor **11**, while **14**, which establishes a single C-H···Cl^- bonding interaction, displays an intermediate chloride affinity between the β,β-**9** and α,α-**17** benzo[*b*]thiophenes. This non-fluorinated α,α-receptor (**17**), binding chloride only through two N-H···Cl^- convergent hydrogen bonds, has the lowest binding constant among the bis-benzo[*b*]thiophenes, despite the high acidic character of its urea binding group. The fluorination of the α-benzo[*b*]thiophene rings in **15**, **16** and **18** naturally leads to an increase in the receptor affinity for chloride, as predicted by the quantum binding descriptors.

Overall, within the benzo[*b*]thiophene-based library, only the fluorinated derivatives showed significant antiport Cl^-/NO_3^- exchange activity. Indeed, the α,β-bis-benzo[*b*]thiophene **15** and the aryl β- and γ-benzo[b]thiophene urea derivatives (**19** and **24**), decorated with -CF_3 substituents, are the most active transporters and follow the sequence **19** > **15** > **24**. These small drug-like molecules share a high lipophilic character (log P values *ca*. 6.0) as well as high acidity for their N-H urea binding units, with E^2 energies of *ca*. 94.4 kcal mol^{-1}, which suggests, that beyond the C-H···Cl^- interactions, these properties may play an important role in the transport activity of these molecules. Moreover, cationophore-coupled assays carried out in the presence of valinomycin or monensin showed that chloride transport mediated by benzo[*b*]thiophene-based molecules is preferentially electrogenic. Further NMDG-Cl assays with gramicidin or oleic acid protonophores confirmed a preferential electrogenic transport pathway, with most of the benzo[*b*]thiophene derivatives promoting chloride efflux *via* a uniport mechanism. Of note, under these conditions, even the α,β-**14** and α,α-**18** derivatives can promote anion transport, yielding relatively low EC_{50} values.

Finally, MD simulations revealed that the transport abilities of these molecules rely on their ability to position themselves at the water/lipid interface and to properly orient their binding units toward bulk water and therefore recognise the solvated anions. In addition, the free energy profiles of three fluorinated derivatives (**15**, **18** and **19**) are comparable, however only molecules with ancillary C-H binding units have any meaningful experimental chloride efflux activity.

With this extensive and comprehensive experimental and theoretical study we have clearly demonstrated how different benzo[*b*]thiophenes isomers modulate anion binding and transport. Given the chemical versatility of the benzo[*b*]thiophene motif, and in-line with our previous findings with the bis-urea series of transporters,[6] this heteroaromatic moiety has become an important addition to the supramolecular designer toolbox, and allows us to fine-tune the binding and transport properties of new synthetic receptors.

Acknowledgement

This work was supported by the projects PTDC/QEQ-SUP/4283/2014 and CICECO–Aveiro Institute of Materials (UIDP/50011/2020), financed by National Funds through the FCT/MEC and co-financed by QREN-FEDER through COMPETE under the PT2020 Partnership Agreement. CM is also thankful to projects UIDB/00100/2020 and UIDP/00100/2020. WGR, L-JC and PAG acknowledge and pay respect to the Gadigal People of the Eora Nation, the traditional owners of the land on which we research, teach, and collaborate at the University of Sydney. PAG thanks the Australian Research Council (DP200100453) and the University of Sydney for funding.

Keywords: Benzo[*b*]thiophene-based thio(urea) Receptors • Anion Binding • Anion Transport • Molecular Modelling • Channel Replacement Therapies

[1] F. M. Ashcroft, *Nature* **2006**, *440*, 440-447.
[2] J. T. Davis, P. A. Gale, R. Quesada, *Chem. Soc. Rev.* **2020**, *49*, 6056-6086.
[3] J. M. Tomich, U. Bukovnik, J. Layman and B. D. Schultz, *Channel Replacement Therapy* for *Cystic Fibrosis - Cystic Fibrosis - Renewed Hopes Through Research*, Sriramulu, D., Ed.; IntechOpen: London, UK, **2012**.
[4] S.-H. Park, S.-H. Park, E. N. W. Howe, J. Y. Hyun, L.-J. Chen, I. Hwang, G. Vargas-Zuñiga, N. Busschaert, P. A. Gale, J. L. Sessler, I. Shin, *Chem* **2019**, *5*, 2079-2098.
[5] I. Carreira-Barral, C. Rumbo, M. Mielczarek, D. Alonso-Carrillo, E. Herran, M. Pastor, A. Del Pozo, M. García-Valverde, R. Quesada, *Chem. Commun.* **2019**, *55*, 10080-10083.
[6] P. Vieira, M. Q. Miranda, I. Marques, S. Carvalho, L. J. Chen, E. N. W. Howe, C. Zhen, C. Y. Leung, M. J. Spooner, B. Morgado, E. S. O. A. B. da Cruz, C. Moiteiro, P. A. Gale, V. Felix, *Chem. Eur. J.* **2020**, *26*, 888-899.
[7] Calculator Plugins were used for structure property prediction and calculation, Marvin Sketch 21.7.0-13120, 2021, ChemAxon (http://www.chemaxon.com).
[8] (a) http://supramolecular.org; (b) D. Brynn Hibbert, P. Thordarson, *Chem. Commun.* **2016**, *52*, 12792-12805.
[9] *Gaussian 09, Revision D.01*, M. J. Frisch, G. W. Trucks, H. B. Schlegel, G. E. Scuseria, M. A. Robb, J. R. Cheeseman, G. Scalmani, V. Barone, B. Mennucci, G. A. Petersson, H. Nakatsuji, M. Caricato, X. Li, H. P. Hratchian, A. F. Izmaylov, J. Bloino, G. Zheng, J. L. Sonnenberg, M. Hada, M. Ehara, K. Toyota, R. Fukuda, J. Hasegawa, M. Ishida, T. Nakajima, Y. Honda, O. Kitao, H. Nakai, T. Vreven, J. A. Montgomery, Jr., J. E. Peralta, F. Ogliaro, M. Bearpark, J. J. Heyd, E. Brothers, K. N. Kudin, V. N. Staroverov, T. Keith, R. Kobayashi, J. Normand, K. Raghavachari, A. Rendell, J. C. Burant, S. S. Iyengar, J. Tomasi, M. Cossi, N. Rega, J. M. Millam, M. Klene, J. E. Knox, J. B. Cross, V. Bakken, C. Adamo, J.

Jaramillo, R. Gomperts, R. E. Stratmann, O. Yazyev, A. J. Austin, R. Cammi, C. Pomelli, J. W. Ochterski, R. L. Martin, K. Morokuma, V. G. Zakrzewski, G. A. Voth, P. Salvador, J. J. Dannenberg, S. Dapprich, A. D. Daniels, O. Farkas, J. B. Foresman, J. V. Ortiz, J. Cioslowski, and D. J. Fox, Gaussian, Inc., Wallingford CT, **2013**.

[10] N. Busschaert, S. J. Bradberry, M. Wenzel, C. J. E. Haynes, J. R. Hiscock, I. L. Kirby, L. E. Karagiannidis, S. J. Moore, N. J. Wells, J. Herniman, G. J. Langley, P. N. Horton, M. E. Light, I. Marques, P. J. Costa, V. Felix, J. G. Frey, P. A. Gale, *Chem. Sci.* **2013**, *4*, 3036-3045.

[11] $E_{complex}$, $E_{receptor}$, and E_{anion} were estimated from the energies of the optimised structures of the complex, free receptor, and chloride corrected for room temperature. The starting geometry of each free receptor was obtained from the respective complex by removing the anion.

[12] (a) Y. Yang, X. Wu, N. Busschaert, H. Furuta, P. A. Gale, *Chem. Commun.* **2017**, *53*, 9230-9233 (b) see also: X. Wu and P. A. Gale, *Chem. Commun.* **2021**, *57*, 3979-3982.

[13] (a) A. Gilchrist, P. Wang, I. Carreira-Barral, D. Alonso-Carrillo, X. Wu, R. Quesada, P. A. Gale, *ChemRxiv* **2021**, DOI 10.33774/chemrxiv-2021-43rq6-v2. This content is a preprint and has not yet been peer-reviewed. (b) X. Wu, P. A. Gale, *J. Am. Chem. Soc.* **2016**, *138*, 16508-16514; (c) X. Wu, L. W. Judd, E. N. W. Howe, A. M. Withecombe, V. Soto-Cerrato, H. Li, N. Busschaert, H. Valkenier, R. Pérez-Tomás, D. N. Sheppard, Y. Jiang, A. P. Davis, P. A. Gale, *Chem* **2016**, *1*, 127-146.

[14] (a) R. Salomon-Ferrer, A. W. Gotz, D. Poole, S. Le Grand, R. C. Walker, *J. Chem. Theory Comput.* **2013**, *9*, 3878-3888; (b) S. Le Grand, A. W. Götz, R. C. Walker, *Comput. Phys. Commun.* **2013**, *184*, 374-380; (c) D. A. Case, S. R. Brozell, D. S. Cerutti, T. E. Cheatham, III, V. W. D. Cruzeiro, T. A. Darden, R. E. Duke, D. Ghoreishi, H. Gohlke, A. W. Goetz, D. Greene, R Harris, N. Homeyer, S. Izadi, A. Kovalenko, T. S. Lee, S. LeGrand, P. Li, C. Lin, J. Liu, T. Luchko, R. Luo, D. J. Mermelstein, K. M. Merz, Y. Miao, G. Monard, H. Nguyen, I. Omelyan, A. Onufriev, F. Pan, R. Qi, D. R. Roe, A. Roitberg, C. Sagui, S. Schott-Verdugo, J. Shen, C. L. Simmerling, J. Smith, J. Swails, R. C. Walker, J. Wang, H. Wei, R. M. Wolf, X. Wu, L. Xiao, D. M. York and P. A. Kollman (**2018**), *AMBER 2018*, University of California, San Francisco.

[15] T. S. Lee, B. K. Radak, A. Pabis, D. M. York, *J. Chem. Theory Comput.* **2013**, *9*, 153-164.

Entry for the Table of Contents

Insert graphic for Table of Contents here.

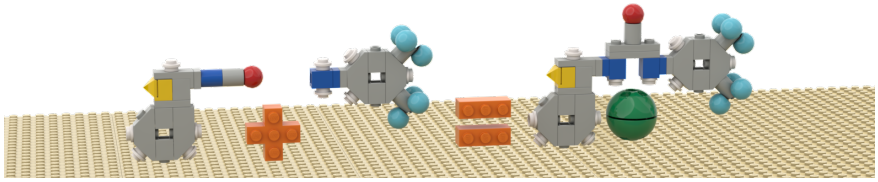

Playing with benzo[b]thiophene-based motifs as Lego bricks, an extensive library of small drug-like synthetic receptors was designed. Their anion binding and transmembrane transport properties were investigated by a combination of experimental and theoretical approaches. The most active transporters recognize chloride using an urea assisted by a C-H binding unit from a single β- or γ-benzo[b]thiophene motif.

Institute and/or researcher Twitter usernames:

CICECO – Aveiro Institute of Materials @ciceco_ua